Impaired neural tube closure, axial skeleton malformations, and tracheal ring disruption in TRAF4-deficient mice

Catherine H. Régnier*†, Régis Masson*, Valérie Kedinger*, Julien Textoris*, Isabelle Stoll*, Marie-Pierre Chenard‡, Andrée Dierich*, Catherine Tomasetto*, and Marie-Christine Rio*§

*Institut de Génétique et de Biologie Moléculaire et Cellulaire, Centre National de la Recherche Scientifique Unité Propre de Recherche 6520/Institut National de la Santé et de la Recherche Médicale Unité 184/Université Louis Pasteur, B.P. 163, 67404 Illkirch Cedex, France; and ‡Service d'Anatomie Pathologique Générale, Centre Hospitalier Universitaire de Hautepierre, 67098 Strasbourg, France

Communicated by David V. Goeddel, Tulank, Inc., South San Francisco, CA, March 4, 2002 (received for review December 12, 2001)

TRAF4 belongs to the tumor necrosis factor receptor-associated factor (TRAF) family of proteins but, unlike other family members, has not yet been clearly associated to any specific receptor or signaling pathway. To investigate the biological function of TRAF4, we have generated *traf4*-deficient mice by gene disruption. The *traf4* gene mutation is embryonic lethal but with great individual variation, as approximately one third of the homozygous mutant embryos died *in utero* around embryonic day 14, whereas the others reach adulthood. Surviving mutant mice manifest numerous developmental abnormalities; notably, 100% of homozygous mutant mice suffer respiratory disorder and wheezing caused by tracheal ring disruption. Additional malformations concern mainly the axial skeleton, as the ribs, sternum, tail, and vertebral arches are affected, with various degrees of penetrance. *Traf4*-deficient mice also exhibit a high incidence of spina bifida, a defect likened to neural tube defects (NTD) that are common congenital malformations in humans. Altogether, our results demonstrate that TRAF4 is required during embryogenesis in key biological processes including the formation of the trachea, the development of the axial skeleton, and the closure of the neural tube. Considering the normal expression pattern of TRAF4 in neural tissues, we can conclude that TRAF4 participates in neurulation *in vivo*.

Cell surface receptors of the tumor necrosis factor receptor (TNFR) and interleukin-1/Toll like receptor (IL-1R/TLR) families are characterized by the lack of enzymatic activities associated to their cytoplasmic domains. Upon stimulation with their respective ligands, these receptors recruit a proximal signaling complex composed of specific adaptor proteins. The recruitment of different signaling molecules allows these receptors to be involved in diverse biological functions including cell proliferation, cell survival, and apoptosis (1, 2).

The TNFR-associated factors (TRAF) belong to one such protein family of cytoplasmic adaptors that interact directly or indirectly with the receptors to mediate the signaling cascade leading to the activation of both the nuclear factor-κB (NF-κB) and the c-Jun N-terminal kinase (JNK) pathways (3). The mammalian genome encodes six TRAF proteins (4, 5). The main structural signature of this family is the well conserved carboxy-terminal TRAF domain, associated with a central repeat of a TRAF-type zinc finger domain, previously defined as CART domain, and an amino-terminal RING finger, both missing in TRAF1 (6). The TRAF domain is responsible for oligomerization of TRAF proteins, binding to receptors, and recruitment of other signal transducers participating in the signaling cascades (3).

The most extensively studied members of the family are TRAF2 and TRAF6, key players involved in the activation of both the NF-κB and JNK pathways. TRAF2 represents the prototypic TRAF protein, which has been reported to be promiscuously recruited to the cytoplasmic domain of all TNFR members (4). The study of *traf2*-deficient mice has confirmed an antiapoptotic function for TRAF2 and its importance in TNF-induced JNK activation (7). In contrast, TRAF6 seems to exhibit more specific functions in CD40 and receptor activator of NF-κB (RANK) signaling by direct receptor binding and also in IL-1R and TLR signaling by interacting with the IL-1R associated kinase. Indeed, defective CD40, RANK, IL-1, and LPS signaling was observed in *traf6*-deficient mice (8).

The human TRAF4 cDNA was initially cloned by a differential screening strategy to identify novel genes associated to breast cancer progression (6, 9). Several classical genetic and biochemical approaches including yeast two-hybrid screens and glutathione *S*-transferase pull-down assays have however failed to specifically link TRAF4 to a known TNFR-signaling pathway (C.H.R. and C.T., unpublished data). Therefore, although the primary structure of TRAF4 protein clearly places it in the TRAF family, the signaling pathway in which the protein is involved remains elusive. Aside from a strong overexpression in about 17% of breast carcinomas, TRAF4 is expressed at a basal level in most adult tissues. Additionally, we previously reported TRAF4 expression throughout mouse embryogenesis, peaking between embryonic day 8.5 (E8.5) and E13.5 (10). More specifically, TRAF4 is expressed during the ontogeny of the central and peripheral nervous systems, in postmitotic undifferentiated neurons. This high level of expression in neuroepithelium suggests a specific role for TRAF4 in neurogenic processes.

Shiels *et al.* (11) have recently generated *traf4*-deficient mice in a mixed 129/SvJ × C57BL/6 genetic background. The mice lacking TRAF4 are viable and are seemingly normal, with the exception of a specific developmental alteration of the upper respiratory tract (11). We concomitantly have generated and analyzed *traf4*$^{-/-}$ mice, and our observations were consistent with this report. Considering that many of the phenotypes examined in mouse models of gene deficiency are influenced by the genetic background in which they are studied (12), we have undertaken further characterization of the targeted *traf4* gene deletion in 129/SvJ inbred mice.

Materials and Methods

Generation of traf4$^{-/-}$ Mice by Gene Targeting. The *traf4* genomic DNA was isolated by screening a 129/SvJ mouse genomic library with the *traf4* cDNA. Genomic clones containing the 5′ start

Abbreviations: TNFR, tumor necrosis factor receptor; TRAF, tumor necrosis factor receptor-associated factor; E*n*, embryonic day *n*; ES cells, embryonic stem cells; MEF, mouse embryonic fibroblast; NTD, neural tube defect; SBO, spina bifida occulta; SBA, spina bifida aperta.

†Present address: Institut National de la Santé et de la Recherche Médicale Unité 255, Centre de Recherches Biomédicales des Cordeliers, 15 Rue de l'Ecole de Médecine, 75270 Paris Cedex 06, France.

§To whom reprint requests should be addressed. E-mail: rio@igbmc.u-strasbg.fr.

The publication costs of this article were defrayed in part by page charge payment. This article must therefore be hereby marked "*advertisement*" in accordance with 18 U.S.C. §1734 solely to indicate this fact.

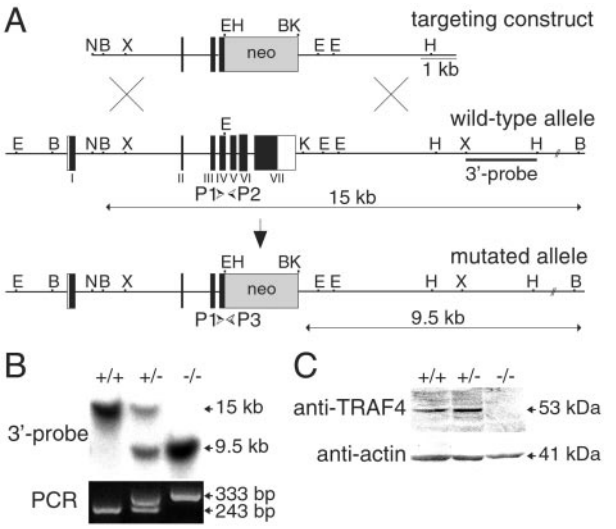

Fig. 1. Targeted disruption of the murine traf4 gene. (*A*) Restriction maps of the targeting construct (*Top*), the *traf4* locus (*Middle*), and the recombinant allele (*Bottom*). The end of exon IV to exon VII is replaced with the PGK-*neo* gene cassette. Translated and untranslated exons are shown as black and white boxes, respectively. The position of the 3′-probe used for Southern blotting and the primers (P1-P3) used for PCR screening are shown. (*B*) Genotyping of *traf4*$^{+/+}$, *traf4*$^{+/-}$, and *traf4*$^{-/-}$ mice. Southern blot analysis (*Upper*) was performed on *Bam*HI-digested tail DNA with the radiolabeled 3′-probe. Arrows indicate the 15-kb wild-type and the 9.5-kb mutant bands. PCR analysis (*Lower*) of yolk sac from E12.5 embryos was carried out by using the primers shown in *A*, generating 243-bp wild-type and 333-bp mutant DNA fragments (arrows). (*C*) Western blot analysis of TRAF4 protein expression. Total protein extracts (40 μg) from *traf4*$^{+/+}$, *traf4*$^{+/-}$, and *traf4*$^{-/-}$ MEFs were analyzed by using an anti-TRAF4 monoclonal antibody. An anti-actin antibody served as a control. Position and molecular weight of the proteins are indicated by arrows.

ATG of *traf4* were analyzed by restriction mapping. The targeting construct was designed to replace the last zinc finger domain and the entire TRAF domain of TRAF4, encompassing exons IV to VII, with the neomycin resistance expression cassette inserted in the same orientation. The 5′ homology arm of the construct consisted of the 3.6-kb *Not*I-*Eco*RI fragment, subcloned into the pPNT vector (13). The 3′ homology arm was a 4.4-kb *Kpn*I-*Xho*I fragment, inserted in pPNT upstream of the thymidine kinase selection cassette. After electroporation with the linearized targeting construct, G418 and gancyclovir-resistant embryonic stem (ES) cell clones were selected. Targeting of the *traf4* locus was determined by Southern blot hybridization with a 2-kb *Xho*I-*Hin*dIII fragment as 3′ probe (Fig. 1*A*). *Bam*HI digestion of genomic DNA generated a wild-type fragment of 15 kb and a recombinant fragment of 9.5 kb. A single insertion of the construct was confirmed by hybridization of a probe specific for the *neomycin*-resistance gene. *Traf4*$^{+/-}$ ES cells were injected into C57BL6/J blastocysts to generate chimeric mice. The resulting male chimeras were backcrossed with 129/SvJ females, and germ-line transmission in F1 *traf4*$^{+/-}$ mice was verified by Southern blot analysis (Fig. 1*B*). Genotyping of F2 mice or embryos was performed on tail or yolk-sac genomic DNA by allele-specific multiplex PCR. The common forward primer (P1: 5′-GCCACTTGAACACTTG-CACGT-3′ located upstream of the disruption site in exon IV) was used in conjunction with two reverse primers specific for the wild-type (P2: 5′-CAGGGGTTAAGTTAGGGGATG-3′ in intron IV) and recombinant (P3: 5′-GCGAAGGGGCCAC-CAAAGAAC-3′ in the *neomycin* gene) *traf4* alleles, generating DNA fragments of 243 and 333 bp, respectively.

Western Blot Analysis of Mouse Embryonic Fibroblasts. *Traf4*$^{+/+}$, *traf4*$^{+/-}$, and *traf4*$^{-/-}$ mouse embryonic fibroblasts (MEFs) derived from E12.5 embryos were prepared and maintained as outlined (14). Primary cultures were harvested in ice-cold PBS, washed twice, and homogenized in lysis buffer containing 20 mM Tris·HCl (pH 7.5), 400 mM KCl, 20% (vol/vol) glycerol, 2 mM DTT, and 0.4 mM PMSF. After a 20-min incubation on ice followed by three freeze-thaw cycles in liquid nitrogen, the cell lysates were centrifuged at 13,000 $\times$ *g* for 15 min, and supernatants were collected. The protein samples were fractionated by SDS/10% PAGE and blotted onto a nitrocellulose membrane. Immunoblot analysis was performed with the anti-TRAF4 monoclonal antibody 5MLN-2H1 raised against the peptide CQSDPGLAKPHVTETFHPD (residues 393–411), as described (6, 15). Protein-antibody complexes were visualized by an enhanced chemiluminescence detection system (DuPont/NEN). To verify that equal amounts of proteins were loaded, blots were reprobed with an anti-actin polyclonal antibody (Santa Cruz Biotechnology, Santa Cruz, CA).

Histological and Skeletal Analyses. Skeletons from newborn and adult mice were prepared to perform staining of cartilage and ossified bone with alcian blue and alizarin red, as described (16). Abnormalities were determined by microscopic observation of cleared preparation of tracheas, ribcages, and spinal columns. Radiographies of anaesthetized adults were obtained by using a Faxitron x-ray system (model MX-20, Faxitron X-Ray, Wheeling, IL). Embryos were collected for analysis between E11.5 and term. Whole embryos and tissues for histology were fixed in Bouin's fixative or in 4% (wt/vol) paraformaldehyde, paraffin embedded, sectioned at 6 μm, and processed for hematoxylin and eosin (H&E) staining.

Results

Generation of TRAF4-Deficient Mice. The cloning and analysis of the murine *traf4* gene showed that, similarly to its human counterpart, it is composed of seven exons (6). A single *traf4* allele was disrupted by targeted homologous recombination into ES cells of 129/SvJ background (Fig. 1*A*). The targeting construct was designed to delete part of exon IV plus exons V to VII, which encode most of the CART domains and the entire TRAF domain (6). Two independent clones of correctly targeted ES cell lines were identified by Southern blot and microinjected into C57BL/6 blastocysts to generate chimeric mice transmitting the mutation in the germline. *Traf4*$^{+/-}$ mice were interbred to obtain homozygosity in the 129/SvJ $\times$ C57BL/6 background. Simultaneously, the male chimeras were backcrossed with 129/SvJ females to generate *traf4*$^{+/-}$ mice and subsequently *traf4*$^{-/-}$ mice in a pure 129/SvJ genetic background. Homozygous mouse mutants derived from the two selected ES cell lines were indistinguishable in all subsequent experiments. Homologous recombination and genotype were checked by Southern blot and PCR analyses (Fig. 1*B*).

To confirm that *traf4*-deficient mice do not express the TRAF4 protein, we prepared primary cultures of MEFs from E12.5 embryos. Whole-cell extracts were analyzed by Western blot with an anti-TRAF4 monoclonal antibody specific of the carboxyl-terminal end of the protein. TRAF4 was detected in both *traf4*$^{+/+}$ and *traf4*$^{+/-}$ MEFs but not in *traf4*$^{-/-}$ MEFs (Fig. 1*C*). No lower molecular mass species, corresponding to carboxyl-terminal truncated translation products from the recombinant allele, were detected with a polyclonal antibody raised against the amino-terminal end of TRAF4 (data not shown).

Embryonic Lethality Induced by TRAF4 Deficiency. Traf4$^{-/-}$ mice in the 129/SvJ $\times$ C57BL/6 background were born alive and at the expected Mendelian frequency (Table 1). However, examination of the progeny from *traf4*$^{+/-}$ parents in the pure 129/SvJ

Table 1. Genotypic analysis of progeny from *traf4*$^{+/-}$ intercrosses

Stage	*Traf4* +/+	*Traf4* +/−	*Traf4* −/−	Total	% −/−
129/SvJxC57BL6					
2 weeks old	50	115	52	217	24
129/SvJ					
E12.5	22	42	26	90	29
E13.5	37	74	37	148	25
E14.5	14	38	10	62	16
2 weeks old	105	206	67	378	18

%, percentage of *traf4*$^{-/-}$ mice.

background revealed a reduced frequency of *traf4*$^{-/-}$ births. Indeed, of 378 live pups examined 2 weeks after birth, only 18% were *traf4*$^{-/-}$ (Table 1). Embryos from timed mating of *traf4*$^{+/-}$ mice were analyzed to determine the time of lethality. *Traf4*$^{-/-}$ embryos died between E13.5 and E14.5 (Table 1). *Traf4*$^{-/-}$ mice that reached adulthood were fertile but their offspring were characterized by an average of three pups per litter, compared with the wild-type average of ten. These observations strongly supported the hypothesis of embryonic lethality associated with the absence of TRAF4 and influenced by the genetic background. Consequently, the rest of our study focused on the characterization of the *traf4*$^{-/-}$ mouse line from the pure 129/SvJ background.

At E14.5, most of the surviving *traf4*$^{-/-}$ embryos showed no obvious morphological abnormalities but appeared smaller than their wild-type littermates. This size difference was maintained to adulthood as both *traf4*$^{-/-}$ female and male mice were approximately 20% smaller in body mass and length (data not shown). The ratio of males to females was unchanged in the *traf4*$^{-/-}$ lineage, and there were no detectable sex-specific differences in the mutant mice. Gross examination of internal organs and tissues, including brain, heart, lung, muscle, palate, liver, pancreas, colon, ovary, uterus, and kidney did not reveal any apparent alterations (data not shown).

Abnormalities of the Upper Respiratory Tract in TRAF4-Deficient Mice. A continuous wheezing sound was detected upon inspiration in *traf4*$^{-/-}$ mice. A similar phenotype was described in *traf4* mutants from a mixed 129/SvJ × C57BL/6 background (11). To further investigate the cause of this phenotype, tracheas from wild-type and mutant newborn and adult mice were stained and macroscopically examined. The upper respiratory tract is composed of the cricoid and the thyroid cartilages, which are the two major components of the larynx, and of segmentally arranged C-shaped cartilaginous rings forming the trachea and extrapulmonary bronchi. In 100% of homozygous mutants analyzed (34 newborns and 35 adults), the trachea displayed an abnormal banding pattern of C-shaped rings, whereas the cricoid and the thyroid cartilages were normal. The tracheal malformations were fully penetrant in *traf4*$^{-/-}$ mice, but their expressivity was variable. Indeed, three to six of the upper tracheal rings below the cricoid cartilage were frontally interrupted and sometimes fused (Table 2 and Fig. 2 *B* and *D*). Histological examinations of sections of E14.5 embryos revealed a striking reduction of the diameter of the tracheal lumen (Fig. 2*F*) compared with wild-type littermates (Fig. 2*E*), confirming the macroscopic observations of stenosis. However, the tracheo-esophageal septum was properly formed. The disorganization of the upper respiratory tract extended to the level of the stem bronchi below the tracheal bifurcation, as lower sections showed that the cartilaginous structure of the extrapulmonary bronchi (Fig. 2*G*) also was malformed and smaller in mutant embryos (Fig. 2*H*).

Table 2. Cartilage and skeletal defects in *traf4*$^{-/-}$ adult mice

Phenotype	Incidence in *Traf4*$^{+/+}$	Incidence in *Traf4*$^{-/-}$	% −/−
Tracheal abnormalities	0/14	35/35	100
TR1 to TR3	0/14	5/35	14
TR1 to TR4	0/14	18/35	51
TR1 to TR5	0/14	10/35	29
TR1 to TR6	0/14	2/35	6
Ribcage abnormalities	0/14	6/35	17
Spina bifida	0/14	14/35	40

TR, tracheal rings. %, percentage of *traf4*$^{-/-}$ mice exhibiting abnormalities.

Rib and Sternum Malformations in TRAF4-Deficient Mice. Examination of cleared skeleton preparations of mutant mice revealed a number of additional skeletal abnormalities (Table 2). In a normal mouse, 13 ribs are dorsally and symmetrically attached on both sides of the vertebrae. The first 7 ribs are vertebrosternebral; i.e., they connect ventrally to the sternum (Fig. 2*I*), whereas the last 6 ribs do not. A normal number of ribs, all attached to the vertebrae, was observed in the mutant mice. However, in about 20% of newborn and 17% of adult *traf4*$^{-/-}$ mice, the ribcage exhibited asymmetrical junctions of the vertebrosternal ribs as well as some lateral fusions (Fig. 2 *J* and *K*). The most common defects corresponded to the fusion of the first and second right ribs on the first intersternebra and the appearance of an eighth vertebrosternal rib on the right side (Fig. 2 *J* and *K*, and data not shown). Additional malformations included the fusion of the fourth and fifth right ribs and irregular sternocostal junctions on the second or third sternebra (Fig. 2 *J* and *K*). In the most severe cases, the shape of the entire sternum was distorted.

Spinal Column Malformations in TRAF4-Deficient Mice. TRAF4 deficiency in mice also resulted in curly tail. Few mice affected by this phenotype survived until adulthood (Fig. 2*L* and data not shown); they were affected in their locomotion and did not reproduce. The curly tail phenotype was coupled to severe skeletal alterations at the level of the spinal column, including scoliosis (Fig. 2 *M* and *N*) and kyphosis (data not shown). Closer examinations of stained mouse skeletons revealed vertebral abnormalities in 100% of mutants with curly tails and in about 40% of all of the *traf4*$^{-/-}$ animals (Table 2). In thoracic, lumbar, and/or sacral vertebrae, the vertebral arches often failed to fuse in the dorsal midline, resulting in a defect of the dorsal structure (Fig. 2 *O* and *P*). Such a malformation corresponds to one form of neural tube closure defects (NTD) named spina bifida occulta (SBO) (17). This phenotype was seen to affect up to six of the lower thoracic and all six lumbar vertebrae in *traf4*$^{-/-}$ mice. The most commonly defective vertebrae were the 12th and 13th thoracic arches that were neither closed nor symmetrical. The opening and asymmetry of the vertebral arches were clearly seen on sagittal sections where the spinal cord was not protected by any dorsal vertebra (Fig. 2 *Q* and *R*). Moreover, intervertebral discs and vertebral bodies were strongly malformed all along the vertebral column. These alterations of the spinal column were more likely a result of the lack of dorsal closure of the vertebrae (Fig. 2*R* and data not shown).

Neural Tube Closure Defect in TRAF4-Deficient Mice. Knowing that the formation of the spinal column is associated to correct neurogenesis and that TRAF4 is expressed in neural tissues as early as E10, we investigated the effect of TRAF4 deficiency on neural development. Some *traf4*$^{-/-}$ embryos isolated from heterozygous intercrosses exhibited another form of NTD, called spina bifida aperta (SBA). This more severe form of failure of spinal cord development affected the caudal end of *traf4*$^{-/-}$

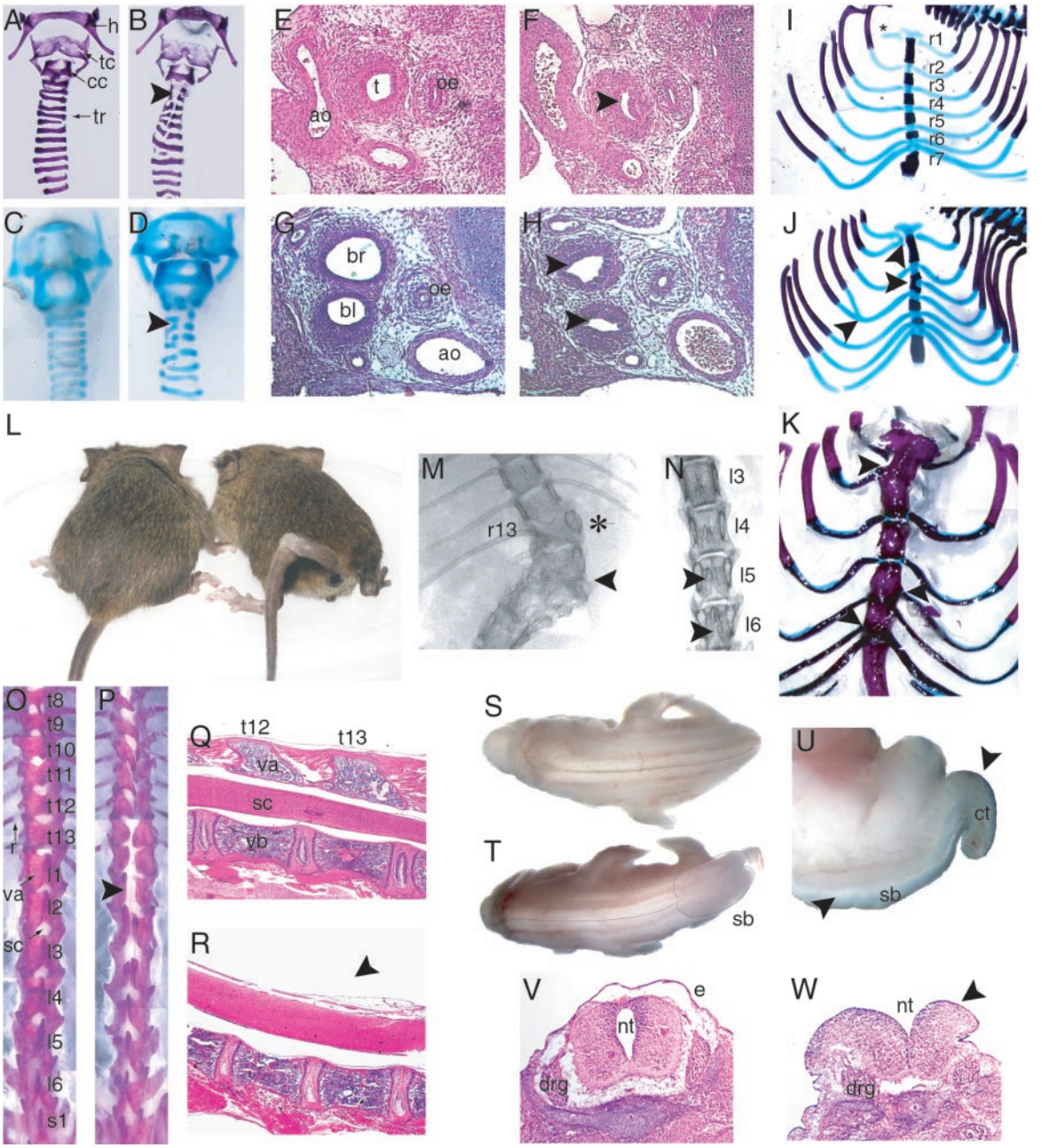

Fig. 2. Cartilage, bone, and neural defects in traf4$^{-/-}$ embryo and adult mice. (*A–D*) Frontal views of *traf4*$^{+/+}$ (*A* and *C*) and *traf4*$^{-/-}$ (*B* and *D*) tracheas and attached hyoid bones from adult (*A* and *B*) and newborn (*C* and *D*) mice. Cartilage staining revealed a focal narrowing of the rostral trachea with disorganization of the C-shaped cartilaginous tracheal rings (tr) (*B* and *D*, arrowheads), resulting in stenosis in all mutant specimens. h, hyoid bone; tc, thyroid cartilage; cc, cricoid cartilage. (*E–H*) Transverse sections of the upper portion of *traf4*$^{+/+}$ (*E* and *G*) and *traf4*$^{-/-}$ (*F* and *H*) tracheas (*E* and *F*) and bronchi (*G* and *H*) from E14.5 embryos. A severe reduction in the lumen diameter of the trachea (t) was observed in mutants (*F*, arrowhead). The malformation of the upper respiratory tree extended below the tracheal bifurcation to the right (br) and left (bl) primary bronchi as the diameter of these structures also was reduced in size (H, arrowheads). ao, aorta; oe, esophagus. (*I–K*) Frontal views of *traf4*$^{-/-}$ rib cages from newborn (*I* and *J*) and adult (*K*) mouse skeletons. Arrowheads (*J* and *K*) indicate multiple fusions of ribs in two mutant mice. r1-r7, vertebrosternal ribs. The incomplete left rib *r* 1 was broken during manipulation (*I*, asterisk). (*L*) Posterior view of two *traf4*$^{-/-}$ adult mice. The animal on the right shows a curly tail phenotype, as observed in several mutant mice. (*M–N*) Dorsal views of *traf4*$^{-/-}$ adult mice analyzed by x-ray. Serious scoliosis is associated with complex bone remodeling (*M*, arrowhead). The 13th right thoracic rib is missing (*M*, asterisk). Observation of bone density of the lumbar vertebrae (l3-l6) revealed a lack of central closure (*N*, arrowheads). (*O–P*) Dorsal overviews of the vertebral columns of *traf4*$^{+/+}$ (*O*) and *traf4*$^{-/-}$ (*P*) adult mice. The vertebral bodies are opened along the spinal column (*P*, arrowhead), reflecting the absence of vertebral arch (va) closure. t8-t13, thoracic vertebrae; l1-l6, lumbar vertebrae; s1, sacral vertebra; r, rib; sc, spinal cord. (*Q* and *R*) Sagittal sections through the vertebral column of *traf4*$^{+/+}$ (*Q*) and *traf4*$^{-/-}$ (*R*) adult mice. Note the complete absence of dorsal vertebral arches (va) to cover the spinal cord (sc) (R, arrowhead). t12-t13, thoracic vertebrae; vb, vertebral body. (*S–U*) Dorsal views of *traf4*$^{+/+}$ (*S*) and *traf4*$^{-/-}$ (*T* and *U*) E13.5 embryos. The dotted line highlights the dorsal vertebral structure. The mutant embryo showed a spina bifida (sb) aperta phenotype (*T*). A close-up view of the caudal region (*U*) shows the unclosed neural tube and the abnormal twisting of the tail bud (arrowheads). ct, curly tail. (*V–W*) Transverse sections of the caudal region of *traf4*$^{+/+}$ (*V*) and *traf4*$^{-/-}$ (*W*) E13.5 embryos. The neural tube (nt) was abnormally open in the mutant embryo and adopted a biconvex configuration exposing the neuroepithelium (*W*, arrowhead). In the mutant, the dorsal ectoderm (e) was absent, and the dorsal root ganglia (drg) appeared displaced laterally and moved downward. (*A–D*, *I–K*, *O–P*) Alcian blue (cartilage) and alizarin red (bone) staining. (*E–H*, *Q* and *R*, *V* and *W*) H&E staining.

embryos (Fig. 2*T*). No such abnormalities were observed in sibling heterozygous or wild-type embryos (Fig. 2*S*). Aside from SBA, irregularly curled tails and wavy dorsal midlines were often detected (Fig. 2*U* and data not shown). At the tissue level, SBA resulted in the exposure of the dorsal neuroepithelium of the embryo (Fig. 2 *V* and *W*). In addition, dorsal root ganglia were abnormally positioned in a more ventral situation (Fig. 2*W*), indicating that not only the central nervous system but also the peripheral nervous system were altered in *traf4*-deficient mice.

To investigate changes in neural tube patterning, a number of molecular markers were tested by *in situ* hybridization on serial sections of E13.5 embryos. Among the 60 single-gene mutations causing NTD in mice, we have analyzed the expression of genes that were potentially connected to TRAF4 because of similar expression pattern and/or phenocopy. These include *sonic hedgehog* (shh), *pax3*, *gli3*, *cartilage homeoprotein 1*, and *traf6* (18, 19). No differences in expression were observed in any of these markers between wild-type and *traf4* mutant embryos (data not shown).

Discussion

The generation of *traf4*-deficient mice in a pure genetic background has revealed important new information on the biological roles of TRAF4. Indeed, TRAF4 deficiency results in embryonic lethality and severe changes in the development of the trachea, the axial skeleton, and the nervous system.

Requirement of TRAF4 for Development of the Trachea. In $traf4^{-/-}$ animals, the C-shaped rings of the upper trachea exhibit specific frontal disruption, lateral fusion, and reduction in diameter. These cartilaginous rings constitute the supporting wall of the trachea and prevent it from collapsing during inspiration. Impaired air passage through the malformed upper respiratory tract results in respiratory distress and wheezing in the mutant animals. The congenital tracheal stenosis is remarkable because it is present in all $traf4^{-/-}$ mice, independently of their genetic background (11), and therefore reveals a specific role for TRAF4 in the formation of tracheal cartilage.

The mechanisms of trachea and lung morphogenesis are known to be governed by reciprocal interactions between epithelial cells derived from foregut endoderm and surrounding mesenchyme. After formation of the respiratory diverticulum around E9.5 in mouse, the mesenchyme induces the migration of the cartilage around the primitive trachea in a segmented, C-shaped fashion, thus forming the tracheal rings (20). The proper development of the cartilaginous rings requires TRAF4 expression not only along the trachea but also at the level of the extrapulmonary bronchi. Our data suggest that the absence of TRAF4 disrupts normal epithelial-mesenchymal interactions in a tightly regulated spatiotemporal manner. The *traf4* gene has a broad pattern of expression during embryonic development (10), including expression in the tracheal epithelium (11). The lack of tracheal ring closure in *traf4*-deficient mice could, therefore, be caused by a defective signal from the tracheal epithelium to the surrounding mesenchyme. Little is known concerning the precise molecular mechanisms governing the formation of the trachea, but analyses of mice deficient for several genes including *retinoic acid receptor* γ (21), *hoxa-5* (22), *nkx2.1* (23), *foxf1* (24), *shh* (25), *gli2* and *gli3* (26) have identified these genes as key players in tracheal development. Considering that most of the genes cited above encode transcription factors, TRAF4 represents the first example of an intracellular signaling molecule essential for tracheal ontogenesis.

Requirement of TRAF4 for Development of the Axial Skeleton. Functional deletion of the *traf4* locus also results in axial skeletal malformations in mouse. The abnormalities concern improper formation of the ribs and more importantly of the vertebral arches, which are dorsally open. Both of these abnormalities indicate a role for TRAF4 in skeletal development and/or cartilage induction.

In vertebrates, the axial skeleton is composed of cartilage and bone produced by paraxial mesoderm (27). Early patterning of the axial skeleton is controlled by genes responsible for the segmentation of paraxial mesoderm into somites and their subsequent differentiation into sclerotomes. Along the embryonic axis, the sclerotomes differentiate to form (dorsally) the vertebral arches and (ventrally) the vertebral bodies and ribs in response to specific inducing factors produced by the neural tube and the notochord, respectively. These factors include Pax3, expressed within the dorsal neural tube and the adjacent somites, and Shh, expressed by the notochord (27).

A number of spinal defects are specifically caused by abnormal induction of the sclerotomes. Defective ventral induction of vertebral bodies on one side of the embryonic axis may result in severe lateral scoliosis, as observed in $traf4^{-/-}$ mice. The abnormal dorsal induction of the vertebral arches also represents one alternative mechanism postulated to cause SBO, the least severe but most common form of vertebral defect. For instance, the *patch* mutant mice that exhibit ribcage abnormalities coupled to SBO are deficient in the *platelet-derived growth factor receptor* α gene, normally expressed in the sclerotome (28). In the case of adult $traf4^{-/-}$ mice affected by SBO, all of the vertebral arches are present, covered by intact skin, but failed to fuse in the dorsal midline, mainly in the lower thoracic and lumbar regions. However, the spinal cord appears to develop normally. These findings would suggest that, in the absence of TRAF4, neural tube closure and sclerotome induction occur, but this latter event is incomplete in specific zones.

Requirement of TRAF4 for Neurogenesis. Further analysis of TRAF4 deficiency revealed a more severe phenotype in some mutant embryos where the caudal region of the neural tube failed to close during neurulation.

Impairment of the genetic program controlling neural development can cause a wide range of abnormalities. NTD are the most frequent congenital malformations in humans, affecting 1 in 1,000 births. In mice, the existence of many NTD-producing genes argues that a number of distinct gene products may be required for neurulation to occur normally (18). In corroboration of the multifactorial nature of NTD, influence of the genetic background and partial penetrance of the phenotype are typically seen in mice bearing a mutation in a single NTD-producing gene (18). Interestingly, these characteristics also are observed in $traf4^{-/-}$ mice.

In a normal embryo, around E8, the lateral edges of the neural plate undergo an elevation process after a rostro-caudal wave (from zone A to D) and converge at the dorsal midline where the edges touch and fuse at four discrete initiation sites. Closure along the remainder of the neural tube proceeds in a zipper-like fashion in defined directions; it is completed on E9 at the head and during early E10 at the base of the tail (17). A failure of the elevation process preceding the closures leads to the most common NTDs, exencephaly and SBA, which correspond to default of elevation of zone B and caudal zone D, respectively (18).

TRAF4 is normally expressed in neuroepithelium and, more specifically, in the neural tube of the developing embryo (10). Considering that a failure of closure of part of the neural tube disrupts both the differentiation of the central nervous system and the induction of the vertebral arches, we can postulate that TRAF4 plays a role in neurulation. Spina bifida is a general term for various degrees of split-spine conditions, ranging from the lack of closure of one or few vertebrae in SBO to the direct exposure of neural tissue, preventing any vertebral arch formation in SBA. In $traf4^{-/-}$ embryos, SBA was observed *in utero*, but

this congenital malformation was never found in newborns, showing that it was embryonic lethal. Some *traf4*$^{-/-}$ embryos with less severe delay of neural-fold elevation in zone D exhibited defect in tail curvature without SBA, but still very few survived. Among the surviving mutant mice, almost half were detected with SBO, indicating that neural tube closure occurred but that the sclerotome induction was impaired. Therefore, both SBA and SBO in *traf4*-deficient mice are very likely to be genetically and developmentally related phenotypes, caused primarily by a neurulation defect rather than a somitic mesoderm abnormality.

A New Role of TRAF Proteins in Neural Development. TRAF4 belongs to the family of TRAF proteins recruited in signaling pathways associated to members of the TNFR and IL-1R/TLR families. Although TRAF4 is a widely expressed protein, detected at a basal level in most tissues and organs as well as during embryonic development, this protein has not yet been clearly associated to any specific receptor or signaling pathway and, therefore, remains an orphan. In this context, it may not be surprising that the phenotype of spina bifida in *traf4*-deficient mice does not closely parallel that of any of the *tnfr*, *il-1r/tlr*, and *traf*-null mutants (29). In particular, mice deficient for *traf1*, *traf2*, *traf3*, *traf5*, or *traf6* gene were mostly affected in the development and maintenance of the immune system (7, 8, 30–32).

Interestingly, further characterization of *traf6*-deficient mice by Lomaga *et al.* (19) has revealed a phenotype of NTD resulting in exencephaly, influenced by genetic background. These authors showed that TRAF6 regulates neural development by controlling the level of programmed cell death within specific regions of the brain during the development of the central nervous system (19). However, the signaling pathway affected during neurulation by the absence of TRAF6 has not yet been characterized.

It is noteworthy to mention that TRAF4 and TRAF6 are the mammalian homologs of dTRAF1 and dTRAF2, two of the three TRAF proteins identified in the *Drosophila* genome (5). The precise role of the TRAF proteins in fly is not yet clearly established, although dTRAF1 was first identified as a signaling molecule interacting with and activating *misshapen*, a Ste20 kinase upstream of the JNK pathway (33). The failure to activate JNK in *Drosophila* leads to embryonic lethality caused by impaired dorsal closure, a phenotype closely related to NTD in mammals.

Together with recent findings, our data strengthen the idea that TRAF4 exerts biological functions distinct from those previously assigned to TRAF proteins and likely to be conserved throughout evolution. As a putative signal transducer, TRAF4 must act in concert with additional factors to influence key steps of neural tube closure. Elucidating how TRAF4 participates in the development of the central nervous system will increase our understanding of the molecular basis of neurulation.

We thank D. J. Heard for critical reading of the manuscript, C. Wendling, M. Oulad-Abdelghani, B. Boulay, P. Eberling as well as the staff of ES cell culture and animal facilities for technical assistance, and O. Lefebvre and G. Gradwohl for helpful discussions. This work was supported by funds from the Institut National de la Santé et de la Recherche Médicale, the Centre National de la Recherche Scientifique, the Hôpital Universitaire de Strasbourg, the Association pour la Recherche sur le Cancer, the Ligue Nationale Française contre le Cancer (LNCC), the LNCC Comités du Haut-Rhin et du Bas-Rhin, the Fondation de France, and the Association Régionale pour l'Enseignement et la Recherche Scientifique et Technologique en Champagne-Ardenne.

1. Locksley, R. M., Killeen, N. & Lenardo, M. J. (2001) *Cell* **104,** 487–501.
2. O'Neill, L. A. & Dinarello, C. A. (2000) *Immunol. Today* **21,** 206–209.
3. Arch, R. H., Gedrich, R. W. & Thompson, C. B. (1998) *Genes Dev.* **12,** 2821–2830.
4. Inoue, J., Ishida, T., Tsukamoto, N., Kobayashi, N., Naito, A., Azuma, S. & Yamamoto, T. (2000) *Exp. Cell Res.* **254,** 14–24.
5. Aravind, L., Dixit, V. M. & Koonin, E. V. (2001) *Science* **291,** 1279–1284.
6. Regnier, C. H., Tomasetto, C., Moog-Lutz, C., Chenard, M. P., Wendling, C., Basset, P. & Rio, M. C. (1995) *J. Biol. Chem.* **270,** 25715–25721.
7. Yeh, W. C., Shahinian, A., Speiser, D., Kraunus, J., Billia, F., Wakeham, A., de la Pompa, J. L., Ferrick, D., Hum, B., Iscove, N., *et al*. (1997) *Immunity* **7,** 715–725.
8. Lomaga, M. A., Yeh, W. C., Sarosi, I., Duncan, G. S., Furlonger, C., Ho, A., Morony, S., Capparelli, C., Van, G., Kaufman, S., *et al*. (1999) *Genes Dev.* **13,** 1015–1024.
9. Tomasetto, C., Regnier, C., Moog-Lutz, C., Mattei, M. G., Chenard, M. P., Lidereau, R., Basset, P. & Rio, M. C. (1995) *Genomics* **28,** 367–376.
10. Masson, R., Regnier, C. H., Chenard, M. P., Wendling, C., Mattei, M. G., Tomasetto, C. & Rio, M. C. (1998) *Mech. Dev.* **71,** 187–191.
11. Shiels, H., Li, X., Schumacker, P. T., Maltepe, E., Padrid, P. A., Sperling, A., Thompson, C. B. & Lindsten, T. (2000) *Am. J. Pathol.* **157,** 679–688.
12. Nadeau, J. H. (2001) *Nat. Rev. Genet.* **2,** 165–174.
13. Tybulewicz, V. L., Crawford, C. E., Jackson, P. K., Bronson, R. T. & Mulligan, R. C. (1991) *Cell* **65,** 1153–1163.
14. Masson, R., Lefebvre, O., Noel, A., Fahime, M. E., Chenard, M. P., Wendling, C., Kebers, F., LeMeur, M., Dierich, A., Foidart, J. M., *et al*. (1998) *J. Cell Biol.* **140,** 1535–1541.
15. Moog-Lutz, C., Tomasetto, C., Regnier, C. H., Wendling, C., Lutz, Y., Muller, D., Chenard, M. P., Basset, P. & Rio, M. C. (1997) *Int. J. Cancer* **71,** 183–191.
16. Dolle, P., Dierich, A., LeMeur, M., Schimmang, T., Schuhbaur, B., Chambon, P. & Duboule, D. (1993) *Cell* **75,** 431–441.
17. Harris, M. J. & Juriloff, D. M. (1999) *Teratology* **60,** 292–305.
18. Juriloff, D. M. & Harris, M. J. (2000) *Hum. Mol. Genet.* **9,** 993–1000.
19. Lomaga, M. A., Henderson, J. T., Elia, A. J., Robertson, J., Noyce, R. S., Yeh, W. C. & Mak, T. W. (2000) *J. Neurosci.* **20,** 7384–7393.
20. Cardoso, W. V. (2000) *Dev. Dyn.* **219,** 121–130.
21. Lohnes, D., Kastner, P., Dierich, A., Mark, M., LeMeur, M. & Chambon, P. (1993) *Cell* **73,** 643–658.
22. Aubin, J., Lemieux, M., Tremblay, M., Berard, J. & Jeannotte, L. (1997) *Dev. Biol.* **192,** 432–445.
23. Minoo, P., Su, G., Drum, H., Bringas, P. & Kimura, S. (1999) *Dev. Biol.* **209,** 60–71.
24. Mahlapuu, M., Enerback, S. & Carlsson, P. (2001) *Development (Cambridge, U.K.)* **128,** 2397–2406.
25. Litingtung, Y., Lei, L., Westphal, H. & Chiang, C. (1998) *Nat. Genet.* **20,** 58–61.
26. Motoyama, J., Liu, J., Mo, R., Ding, Q., Post, M. & Hui, C. C. (1998) *Nat. Genet.* **20,** 54–57.
27. Olsen, B. R., Reginato, A. M. & Wang, W. (2000) *Annu. Rev. Cell Dev. Biol.* **16,** 191–220.
28. Payne, J., Shibasaki, F. & Mercola, M. (1997) *Dev. Dyn.* **209,** 105–116.
29. Yeh, W. C., Hakem, R., Woo, M. & Mak, T. W. (1999) *Immunol. Rev.* **169,** 283–302.
30. Tsitsikov, E. N., Laouini, D., Dunn, I. F., Sannikova, T. Y., Davidson, L., Alt, F. W. & Geha, R. S. (2001) *Immunity* **15,** 647–657.
31. Xu, Y., Cheng, G. & Baltimore, D. (1996) *Immunity* **5,** 407–415.
32. Nakano, H., Sakon, S., Koseki, H., Takemori, T., Tada, K., Matsumoto, M., Munechika, E., Sakai, T., Shirasawa, T., Akiba, H., *et al*. (1999) *Proc. Natl. Acad. Sci. USA* **96,** 9803–9808.
33. Liu, H., Su, Y. C., Becker, E., Treisman, J. & Skolnik, E. Y. (1999) *Curr. Biol.* **9,** 101–104.